

Kinetic instability of a chitosan – aspartic acid – water system as a method for obtaining nano- and microparticles



T.N. Lugovitskaya ^{a*} , A.B. Shipovskaya ^b, X.M. Shipenok ^b

a: Ural Federal State University named after the first President of Russia B. N. Yeltsin, 620002 Mira st., 19, Yekaterinburg, Russia

b: Saratov National Research State University named after N.G. Chernyshevsky, 410012 Astrakhanskaya st., 83, Saratov, Russia

* Corresponding author: tlugovitskaja@mail.ru

This article belongs to the regular issue.

© 2021, The Authors. This article is published in open access form under the terms and conditions of the Creative Commons Attribution (CC BY) license (<http://creativecommons.org/licenses/by/4.0/>).

Abstract

The specific electrical conductivity and dielectric constant of aqueous solutions of ionic aminopolysaccharide chitosan in *L*-aspartic acid were investigated. An increase of the mobility of charge carriers in these solutions was found in comparison with solutions of an individual acid. The evaluation of the kinetic stability revealed that the viscosity, electrical conductivity and dielectric constant of the chitosan – *L*-aspartic acid – water system decrease, while the pH value increases. It was shown that the time variation of physicochemical and electrochemical parameters is due to the effects of counterionic association with the transition of macromolecules to the ionomeric state and is accompanied by phase segregation of the polymer phase in the form of nano- and microparticles. The conducted studies carried out have shown the fundamental possibility of controlling the metastable state of this system in order to obtain nano- and microparticles.

Keywords

chitosan
L-aspartic acid
counterionic
association
nanoparticles

Received: 06.10.2021

Revised: 20.11.2021

Accepted: 23.11.2021

Available online: 26.11.2021

1. Introduction

Chitosan (CTS), a product of partial or complete deacetylation of chitin, is an ionic copolymer of aminopolysaccharide. Since the temperature of thermal decomposition of CTS is lower than its melting point, the processing of this polymer into the final products involves the step of dissolving in organic or inorganic acids. In an aqueous acidic medium at pH below pK_a , the amino groups of CTS are protonated, resulting in the formation of a salt form of the polymer – a positively charged polyelectrolyte ($\sim -NH_3^+$) with ionic conductivity. The main contribution to the transfer of electricity in an aqueous acidic CTS solution is made by free counterions, as well as excess of hydronium ions [1–3]. In this case, the nature of the acid-solvent of CTS significantly affects the quantitative characteristics of electrical conductivity, which determines the conformation of macromolecules in solution and the phase state of the polymer system after removal of the liquid medium [1]. Thus, in strong HCl, a linear decrease in the specific electrical conductivity (σ_{sp}) with an increase in the CTS concentration (C_{CTS}) is observed. The conformation of the expanded helix is realized due to the repulsion of charged macrochains. In weak acids (propionic, acetic and

formic), the concentration dependence of the specific electrical conductivity is nonlinear, the σ_{sp} values grow increase with an increase in C_{CTS} value. There is an attraction and “adhesion” of local sections of macrochains through ionic crosslinking $\sim -NH_3^+$ with $R - COO^-$ and H-bonds of OH-groups of CTS with the carbonyl oxygen of the acid, as a result of which the macromolecules assume the coiled conformation. CTS solutions in HCl have a weak film-forming ability and give a loose structure with a pore diameter of more than 10 nm when dried on an inert surface. CTS films cast from aqueous solutions of carboxylic acids are characterized by a dense ordered structure.

When an electric field is applied in an aqueous acidic CTS solution, internal polarization phenomena can occur, i.e., displacement of charges that create a volume-distributed dipole moment. The relaxation processes of the electric polarization of the CTS salt form are manifested in dielectric spectra in the frequency range below 1010 Hz [4]. Like conductometry, dielectric relaxation spectroscopy is highly sensitive to changes in the electrical conductive properties of aqueous acidic CTS solutions and makes it possible to reliably control the state of counterions (free, bound) in them.

CTS macromolecules are characterized by highly complex behavior in solutions. This is primarily due to the polyelectrolyte swelling of charged macromolecular coils and increased chain rigidity. CTS solutions are also characterized by instability of viscosity properties over time, which is usually explained by the destruction of macromolecules as a result of acid hydrolysis of glycosidic bonds [5–7]. However, there are studies that make it possible to exclude destruction as the main reason for the decrease in the viscosity of chitosan solutions in time [8, 9] and to explain this effect by conformational rearrangements of macromolecules [10], changes in the supramolecular structure, including aggregation [9, 11], and also by phase separation of the system as it is stored [11, 12].

CTS is widely used due to a complex of valuable properties, as well as an annually renewable resource base [13–15]. Chitosan-containing nanomaterials, in particular nanoparticles, deserve special attention [16, 17]. Compared to the original CTS, they acquire additional valuable properties due to their small size, increased surface area, and quantum size effects. Like CTS, chitosan-containing nanoparticles are non-toxic, biocompatible, and biodegradable, which predetermines their use in medicine, as well as in the food, textile, and cosmetic industries [18–22]. For obtaining nanoparticles, the most common used are spray drying under special conditions, or methods of ionotropic gelation and emulsion cross-linking with tripolyphosphate, glutaraldehyde, genipin [16]. In some cases, dibasic and tribasic pharmacopoeial acids (malic, tartaric, citric, and succinic) were used, which simultaneously act as a solvent for the polymer and as a cross-linking reagent [23–25]. It should be noted that the use of biologically active acids for the formation of CTS nanoparticles significantly expands the directions of their application in biomedical and pharmacological applications [26–28], veterinary medicine [29], and plant growing [30–33].

The use of *L*-aspartic acid (AspA), a proteinogenic amino acid that plays an important role in a living organism, seems to be promising [34, 35]. Unlike traditional water-acid CTS dissolving media based on monobasic carboxylic acids (HCOOH , AcOH), AspA contains two carboxylic and one amino groups. Therefore, in an aqueous solution, depending on the pH of the medium, its molecules can exist in several ionic forms. At $\text{pH} = 3.0$, the isoelectric point is located, at $\text{pH} = 4$, almost equal proportions of zwitter ions (H_2Asp) and aspartate anions (HAsp^-) are realized, whereas in the range of $\text{pH} = 4.7\text{--}8.0$, HAsp^- is the predominant ion [36]. The resulting high concentration of hydrogen ions (hydronium), which are the main carriers of electricity, provides prototropic conductivity of an aqueous solution of AspA [37, 38].

Previously, we have found that the solubility of AspA in H_2O increases in the presence of CTS [39]. The conditions for the preparation of CTS solutions in AspA – H_2O mixture and some of their properties have also been discussed [40]. Thus, in an aqueous medium, the macromolecules of the salt CTS form exhibit the properties of a weak-

ly dissociating polyelectrolyte with a partially compensated charge. The calculated Huggins constants and temperature viscosity coefficients showed an increased rigidity of their macrochains. However, kinetic stability was not evaluated, although the CTS – AspA – H_2O system showed all the characteristic features of phase separation. As in the case of synthetic polyelectrolytes [41, 42], not only the dissociation of ionogenic groups of CTS aspartate can occur in an aqueous medium, but also the interaction of the polycation with HAsp^- with the formation of ion pairs, multiplet structures (combination of ion pairs) and the transition of macromolecules to the ionomeric state. At the initial stage of phase separation, these processes should be accompanied by phase segregation of the polymer phase in the form of nano- and microparticles. This assumption served as the basis for this study.

The aim of this work is to study the kinetic stability of the CTS – AspA – H_2O system during storage to obtain nano- and microparticles using viscometry, potentiometry, conductometry, and dielectric relaxation spectroscopy as the most informative methods for studying the counterions state (free, bound) in polyelectrolyte solutions [4, 40–42].

2. Materials, objects and methods

2.1. Materials

The starting reagents were powdered CTS with a viscosity-average molecular weight $\bar{M}_v = 200$ kDa, a degree of deacetylation of 82 mol%, and a moisture content of $W = 8 \pm 1$ wt% (ZAO Bioprogress, RF); powdered *L*-AspA of pharmacopoeial purity, obtained by biocatalytic synthesis using *E. coli* strain VKPM 7188 (JSC Bioamid, RF); distilled water ($\text{pH} = 6.0$); ethyl alcohol (95.6%), and acetone (99.8%). CTS and AspA were used without additional purification; all other reagents were of analytical grade.

2.2. Preparation of objects of study

A working AspA solution with a concentration of $C_{\text{AspA}} = 0.06$ mol/L was prepared by dissolving a weighed portion of AspA powder in distilled water at 80 °C, followed by cooling down to room temperature at a rate of 20 °C/h. A series of solutions of lower concentrations were obtained by successive dilution of the working solution with distilled water. The pH values of AspA solutions in H_2O with $C_{\text{AspA}} = 0.003\text{--}0.060$ mol/L were in the range of 3.1–4.2. Freshly prepared acid solutions were used in all experiments.

To obtain system CTS + AspA + H_2O , calculated weighed portions of CTS (considering the moisture sample) and AspA were placed into some volume of H_2O and stirred on a magnetic stirrer at a rotation speed of 400–500 rpm at 25 °C until visual dissolution of the powders (for 2–3 h). The concentrations of the polymer and acid in the solution were varied in the ranges $C_{\text{CTS}} = 0.002\text{--}0.035$ monomol/L and $C_{\text{AspA}} = 0.03\text{--}0.06$ mol/L, respectively. Before experiments, all systems were filtered through a Millipore filter with a pore diameter ≤ 0.45 μm.

The CTS + AspA + H₂O system were stored in a room atmosphere (760 mm Hg, 22±2 °C) for 96 h, regularly taking samples to assess their physicochemical parameters. In all experiments, the conditions for the preparation of the system and the time at which the physicochemical characteristics began to be measured were the same. The stability of the systems was assessed by measuring their conductivity, pH, viscosity and permittivity, as well as by SEM.

2.3. Obtaining particles

To obtain nanoparticles and microparticles, 0.5 μL of a freshly prepared or stored CTS + AspA + H₂O system was sprayed onto a degreased (ethyl alcohol, acetone) glass surface using a mechanical syringe-shaped injector and dried for 1–2 h (the technique is similar [43]). The obtained particles obtained were dried at 22±2 °C under atmospheric pressure to an air-dry state, and analyzed using SEM.

2.4. Methods

Gravimetric measurements were carried out on an Ohaus Discovery analytical balance (USA), weighing accuracy being ±0.0001 g.

pH was measured on a Mettler Toledo Five Easy FE20 pH-meter (MTD, Singapore).

Conductivity was measured on a WTW inoLab Cond 7110 conductometer (Germany) at 25 °C. A thermostated cell with a volume of 25 mL was used. Specific conductivity (α_{sp} , S·m⁻¹) was calculated using the specific conductivity of water by the formula:

$$\alpha_{sp} = K/R - \alpha_{H_2O} = \alpha_{CTS} - \alpha_{H_2O}, \quad (1)$$

where $K = 0.1213 \text{ m}^{-1}$ is the cell constant evaluated from 0.01 N KCl solution; R is the resistance of the system, S; α_{CTS} and α_{H_2O} are the specific conductivity of the chitosan-containing system and water, respectively, S·m⁻¹.

The viscometric measurements were carried out in an Ubbelohde viscometer (RF) with a capillary diameter of 0.56 mm at 25 °C. The relative viscosity (η_{rel}) was calculated from:

$$\eta_{rel} = t/t_0, \quad (2)$$

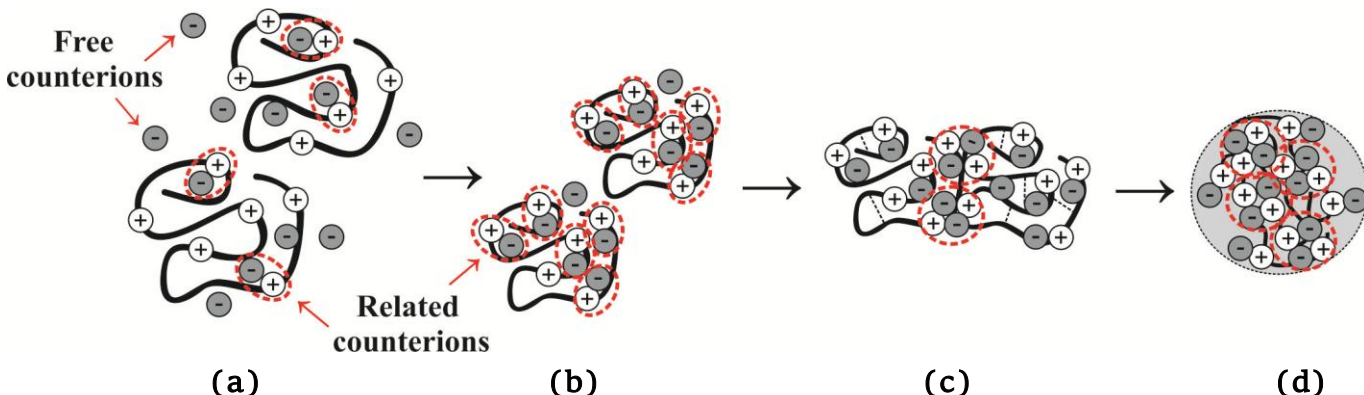


Fig. 1 Distribution of free and bound counterions in the CTS - AspA - H₂O system during storage: (a) polycation with a partially compensated charge, (b) ion pairs, (c) multiplets, (d) phase segregation of the polymer phase in the form of a nanoparticle

where t is the flow time of the CTS + AspA + H₂O systems, s; t_0 is that of the AspA aqueous solution, s; C_{CTS} is expressed in g/dL; the accuracy of measuring t and t_0 was ±0.1 s.

The frequency dependences of the real (ϵ') and imaginary (ϵ'') parts of the complex permittivity were measured on an Agilent Microwave Network Analyzer PNA-X N5242A vector network analyzer (USA) using an Agilent 85070E coaxial probe in the frequency range $f = 10^7$ – 10^{11} Hz at 25 °C. The dielectric loss tangent was calculated from the ratio $\operatorname{tg}\delta = \epsilon''/\epsilon'$.

SEM images were taken on a MIRA\LMU scanning electron microscope (Tescan, CZ) equipped with an energy dispersive detector (EDX) at a voltage of 30 kV and a conducting current of 400 pA. A 5 nm thick gold layer was deposited on each sample using a K450X Carbon Coater (DE).

2.5. Statistical analysis

In each experiment on the study of physicochemical properties, at least 3 parallel experiments were carried out; the arithmetic mean and standard deviation were calculated.

3. Results and discussion

We have previously shown that the concentration dependence of the reduced specific viscosity of a freshly prepared aqueous solution of CTS aspartate is not linear, has a max or a plateau and a descending branch with a decrease in CTS [40]. This hydrodynamic behavior indicates the implementation of a mixed polyelectrolyte-ionomer mode, when some of the HAsp⁻ counterions are in an associated (bound) state with $-\text{NH}_3^+$ groups of the macrochain with the formation of ion pairs (Fig. 1a).

The revealed features of the counterions state in macromolecular coils of the CTS salt form were proved by studying the electrochemical properties of the polymer system.

Thus, the specific electrical conductivity of a CTS solution in AspA - H₂O at $C_{CTS} = \text{const}$ increases with an increase in the acid concentration (Fig. 2a, curve 1). A similar dependence is observed for aqueous solutions of individual AspA (curve 2).

The revealed features of the counterions state in macromolecular coils of the CTS salt form were proved by studying the electrochemical properties of the polymer system. Thus, the specific electrical conductivity of a CTS solution in AspA - H₂O at $C_{CTS} = \text{const}$ increases with an increase in the acid concentration (Fig. 2a, curve 1). A similar dependence is observed for aqueous solutions of individual AspA (curve 2). It is noteworthy that at $C_{AspA} < 0.01 \text{ mol/L}$, the increase in α_{sp} values of both AspA - H₂O and CTS solutions in AspA - H₂O is practically proportional to the increase in C_{AspA} . In this case, despite the protonation of the amino groups of the macrochains in an aqueous acidic medium and, as a consequence, the binding of the labile H⁺ of the carboxyl group to the NH₂ moiety of the polymer, the α_{sp} values of aqueous solutions of CTS aspartate and AspA are the same. Taking into account that the electrical conductivity is determined by the number of charged particles and their mobility [1–3], this character of the dependence $\alpha_{sp} = f(C_{AspA})$ for a polymer solution can be explained by shifting acid-base equilibrium towards the acid in the presence of CTS (base). As a result of ionization of previously undissociated AspA molecules, the concentration of H⁺ and HAsp⁻ ions increases, and the total amount of free ions (electricity carriers) in solutions of CTS in AspA - H₂O and AspA in H₂O remains constant. At $C_{AspA} > 0.01 \text{ mol/L}$, the rate of increase in the specific conductivity of the CTS solution slightly decreases and the α_{sp} values become lower than that of individual AspA, which may be due to a decrease in the degree of acid dissociation as it is concentrated in the solution. However, an increase in α_{sp} value with an increase in the acid concentration in this C_{AspA} range also indicates the intensification of AspA protolysis in an aqueous acid solution of CTS, although to a lesser extent compared to the range of $C_{AspA} < 0.01 \text{ mol/L}$. The proposed explanation of the associative-dissociative processes is also confirmed by the data in Fig. 2b, if we consider the dependence $\alpha_{sp} = f(C_{CTS})$ at $C_{AspA} = \text{const}$. In addition, a significant increase in the specific electrical conductivity with an increase in C_{CTS} at $C_{AspA} = \text{const}$ indicates an increase in the mobility of conductive particles not only in comparison with an aqueous solution of AspA, but also in comparison with H₂O. Note that a nonlinear increasing dependence $\alpha_{sp} = f(C_{CTS})$ has also been observed in CTS solutions in weak propionic, acetic, and formic acids [1].

The evaluation of the dielectric properties also showed an increase in the mobility of the electrically transporting particles in the CTS aspartate solution. It is noteworthy that in the frequency range of $f < 10^9 \text{ Hz}$, the real part of the complex dielectric constant of CTS solutions in AspA-H₂O mixture is less than ϵ' of an aqueous solution of AspA and water (Fig. 3a), and the dielectric loss factor and dielectric loss tangent are larger (Fig. 3b, c). The ϵ' values decrease, ϵ'' and tgδ values increase with an increase in C_{CTS} . Consequently, in CTS solutions in AspA-H₂O mixture there is a larger amount of mobile charge carriers providing ohmic current than in AspA-H₂O and aqueous solutions. At $f > \sim 1.6\text{--}1.8 \cdot 10^9 \text{ Hz}$, the

ϵ' , ϵ'' , and tgδ values of aqueous solutions of CTS aspartate, AspA and water are comparable. This character of the dispersion of ϵ' , ϵ'' , and tgδ values of a solution of CTS aspartate is explained by the fact that at high frequencies a “fast” mechanism of ion polarization is realized, the large sizes of macrocoils prevent the movement of macrodipoles (associations of polar groups of a polymer molecule through dipole-dipole interaction) in an alternating electric field and the electric induction of the system is determined only by the mobility of low molecular weight ions [4]. As f value decreases, the “slow” mechanism of orientational (dipole) polarization occurs, and the possibility of the macrodipoles motion, accompanied by dissipative losses, appears. The smaller f values, the greater are the dielectric losses (ϵ'' , tgδ), since the macrodipoles have more time to orient themselves along the electric field.

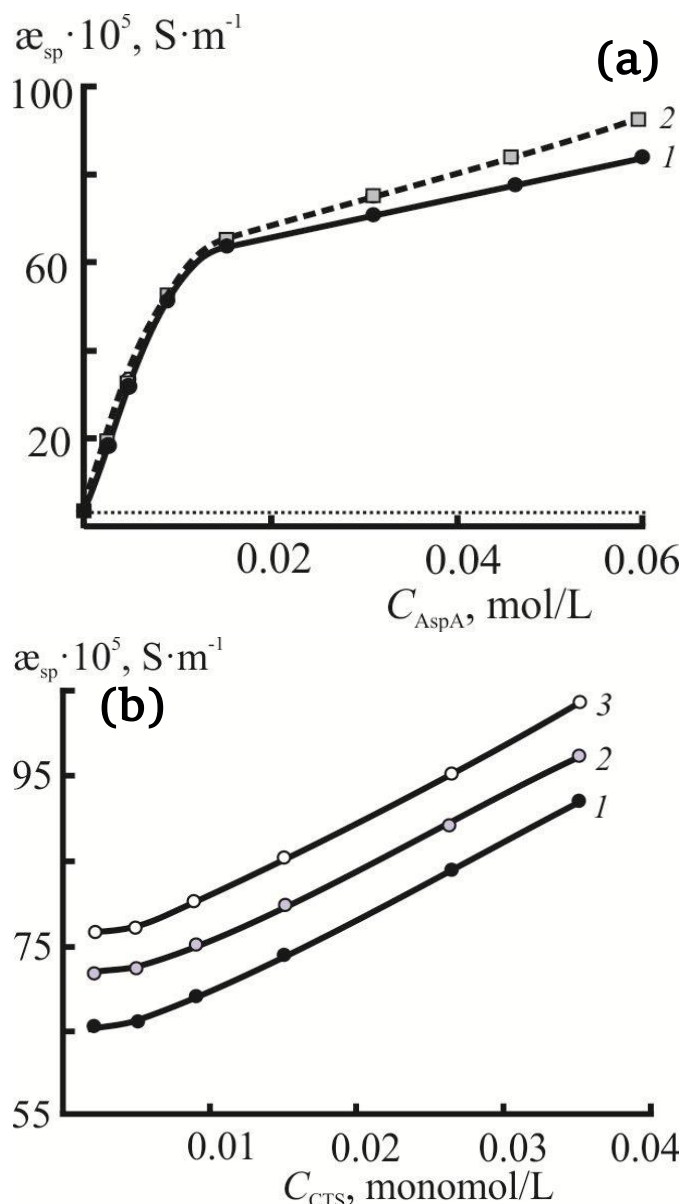


Fig. 2 Dependence of the electrical conductivity of CTS solutions in AspA-H₂O mixture with $C_{CTS} = 0.015 \text{ monomol/L}$ (1a) and AspA aqueous solution (2a) on AspA concentration, as well as CTS solutions in AspA-H₂O mixture with $C_{AspA} = 0.030$ (1 b), 0.045 (2b) and 0.060 mol/L (3b) on CTS concentration; the dotted line shows α_{sp} value for water

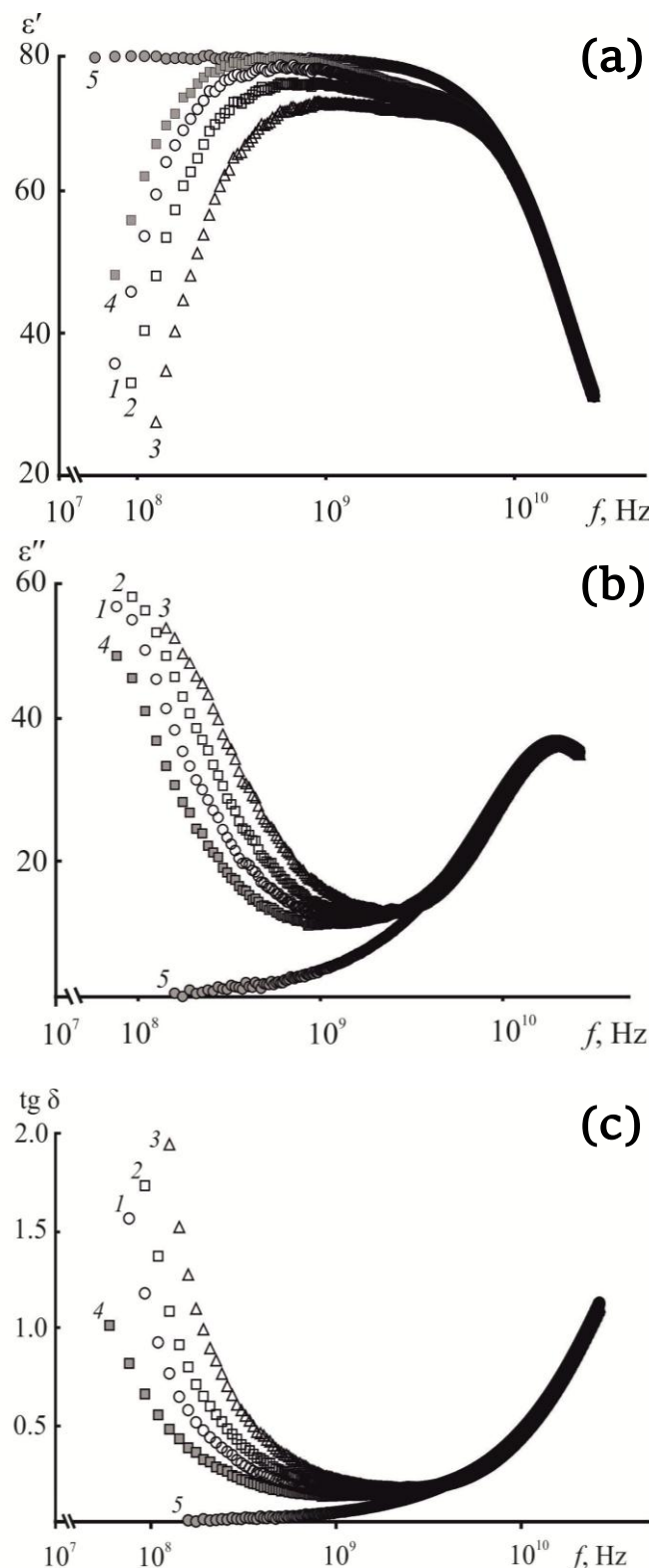


Fig. 3 Dispersion of the real part of the complex dielectric constant (a), dielectric loss factor (b) and dielectric loss tangent (c) of CTS solutions in AspA - H₂O mixture with $C_{\text{AspA}} = 0.030$ mol/L and $C_{\text{CTS}} = 0.010$ (1), 0.018 (2) and 0.035 monomol/L (3), as well as AspA - H₂O mixture with $C_{\text{AspA}} = 0.030$ (4) and water (5)

The high mobility of charged particles in a solution of CTS aspartate was reflected in the kinetic stability of the polymer system. It turned out that exposure at room atmosphere is accompanied by a significant decrease in the relative viscosity of CTS solutions in AspA-H₂O mixture and

an increase in the medium acidity (Fig. 4a, curves 1 and 2). These changes are most intense in the first ~ 16–18 hours after preparation of the solution and increase with increasing CTS concentration. So, after 24 hours of storage of solutions with $C_{\text{CTS}} = 0.002$ –0.006 monomol/L, the effect of reducing η_{rel} was 7–10%, and 23% (Fig. 4a, curve 1) for more concentrated solutions, for example, with $C_{\text{CTS}} = 0.035$ monomol/L.

In addition, during storage for ~16 – 18 hours in a visually homogeneous solution of CTS in AspA – H₂O mixture, the specific conductivity increases (Fig. 4b, curve 3). The dielectric constant in the frequency range of $f < 10^9$ Hz decreases, and in the range of $f > 1.8 \cdot 10^9$ Hz it increases with a local maximum (curves 4 and 5). At $t > 24$ hours, opalescence α_{sp} value begins to decrease with the realization of lower values than in a freshly prepared solution; ϵ' value decreases with time over the entire range of f . Like η_{rel} value, in this case, the α_{sp} and ϵ' values change to the greater extent, the higher the polymer concentration in the system. After ~66–74 hours the phase separation occurs, which is observed visually as the precipitation of a water-insoluble fine sediment.

Like relative viscosity, specific electrical conductivity and dielectric constant change with time to the greater extent, the higher the polymer concentration, and pH – vice versa. For example, for a system with $C_{\text{CTS}} = 0.035$ monomol/dL, during ~50–60 days of storage the values of these parameters change in the range of $\alpha_{\text{sp}} = (92\text{--}88) \cdot 10^{-5}$ S·m⁻¹, $\epsilon' = 38\text{--}22$ ($f = 1.2 \cdot 10^8$ Hz), pH = 4.9–5.0, and for a system with $C_{\text{CTS}} = 0.002$ monomol/dL – $\alpha_{\text{sp}} = (60\text{--}58) \cdot 10^{-5}$ S·m⁻¹, $\epsilon' = 72\text{--}64$ and pH = 3.1–3.2. The shortest time interval before the precipitation of the polymer phase is also observed at a higher C_{CTS} .

At first glance, a decrease in the viscosity of the system under study with time may be associated with the macromolecules destruction as a result of acid hydrolysis of glycosidic bonds [5–7], and an increase in pH is due to deprotonation of AspA with the transition of some of the acid molecules into the zwitterionic H₂Asp form. However, upon destruction with a decrease in the molecular weight of CTS, the amount of free counterions and hydronium ions should increase, and the pH value should decrease. As a result, the destructive processes should lead to an increase in ionic conductivity, i.e., electrical conductivity and dielectric constant should increase monotonically, but not very significantly. Since for the CTS – AspA – H₂O polyelectrolyte system under study a different character of the α_{sp} and ϵ' kinetics is observed, it seems that its instability in time is associated with the effects of the association of counterions with protonated amino groups of the polycation and their further transformations. Probably, it is thermodynamically not favorable for counterions to be in a free state, and they continue to form ion pairs with $-\text{NH}_3^+$ groups of polymer chains (ionomers), while losing in entropy, but gaining in electrostatic energy (Fig. 1b).

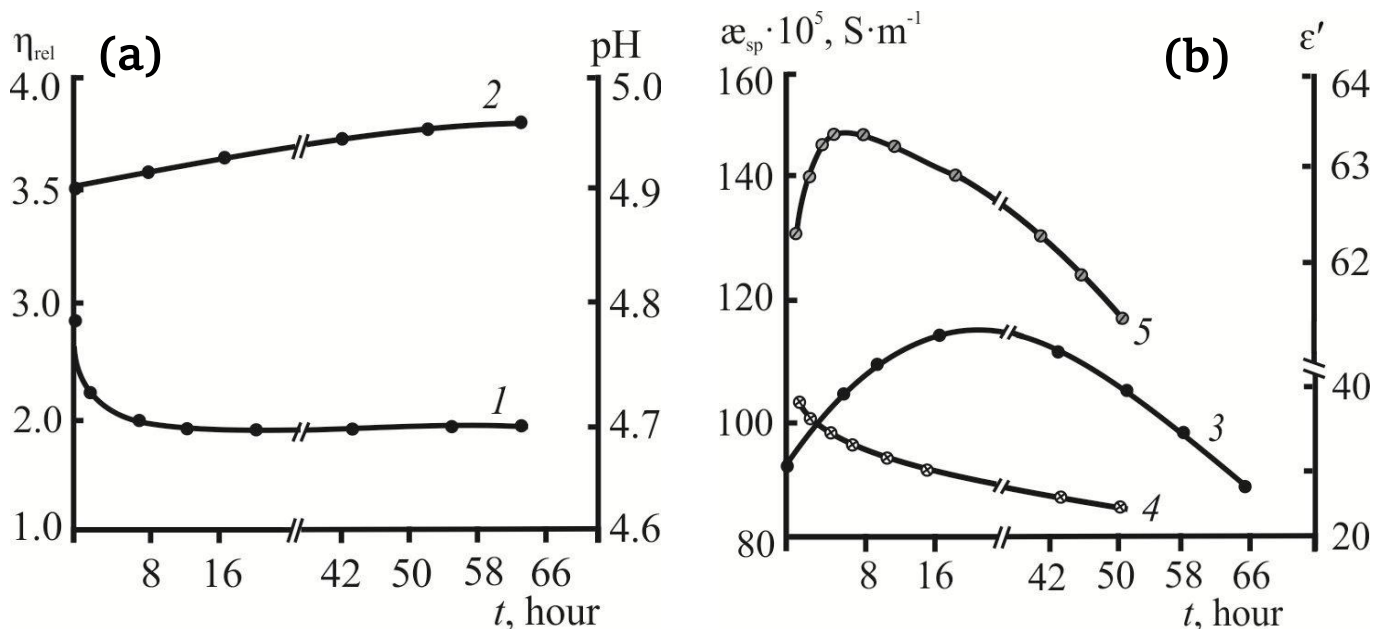


Fig. 4 Kinetic dependences of the relative viscosity (1a), pH (2a), specific electrical conductivity (3b) and dielectric constant at $f = 1.2 \cdot 10^8$ (4b) and 10^{10} Hz (5b) of the CTS – AspA – H₂O system with $C_{\text{CTS}} = 0.035$ monomol/L, $C_{\text{AspA}} = 0.030$ mol/L

The transition of counterions from the aqueous medium to the macrocoil volume leads to screening of electrostatic repulsion between the like-charged links of the macrochain, a decrease in α_{sp} , η_{rel} , and ϵ' values of the system and, accordingly, its transition to the ionomic mode. The resulting effective attraction between monomer units contributes to the dipole-dipole interaction of ion pairs and their combination into multiplet structures (Fig. 1c). Most likely, the stabilization of the latter occurs through complex ion-ion-hydrogen contacts of ionogenic groups of the CTS aspartate macromolecule and the AspA molecule (the possibility of the formation of such CTS-

acid contacts has been reported in [1]). Multiplets function as physical crosslinks between different polymer chains, which contributes to the compaction of macrocoils and the formation of nanosized nuclei of a new phase (Fig. 1d). Upon aggregation of the latter to micro- and macroparticles, the metastable polymer system is divided into two equilibrium phases: the polymer-rich phase precipitates, the polymer-depleted phase is represented by the supernatant liquid. According to [41], phase separation in a polyelectrolyte solution under conditions of ionic association can occur even in a thermodynamically good solvent.

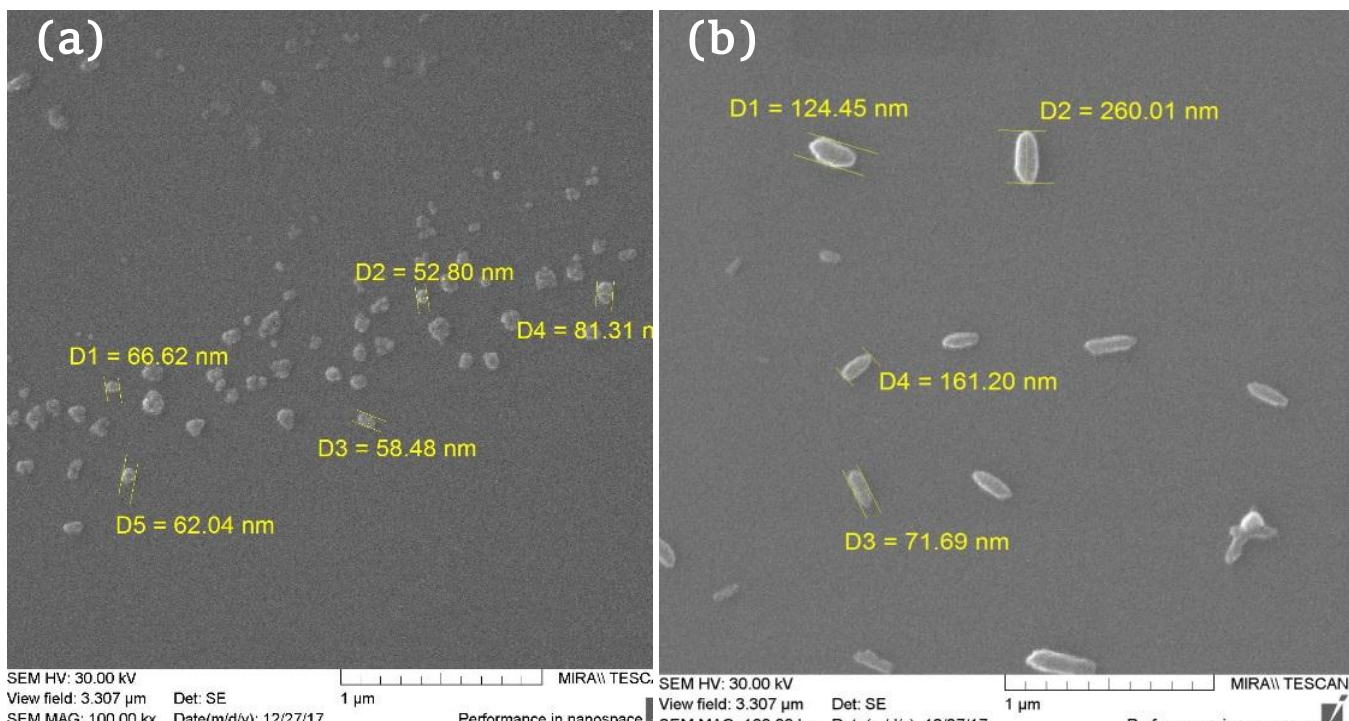


Fig. 5 SEM image of particles isolated from the CTS-AspA-H₂O system with $C_{\text{CTS}} = 0.035$ monomol/L, $C_{\text{AspA}} = 0.030$ mol/L after 24 (a) and 36 hours (b)

The described associative processes were confirmed and visualized using scanning electron microscopy. For example, in a CTS – AspA – H₂O sample, spherical nanoparticles with a size of $d = 40\text{--}90$ nm (Fig. 5a) and ellipsoidal ones with a size of $d = 70\text{--}260$ nm (Fig. 5b) were revealed after 24 and 36 hours, respectively. After ~48–70 hours, the average size of chitosan-containing particles was ~1.4–2.0 μm , width was ~0.6–0.8 μm ; their aggregation was also observed.

Elemental analysis data showed that the nanosized polymer phase contains $42.95 \pm 1.2\%$ carbon, $21.09 \pm 0.9\%$ nitrogen, and $35.96 \pm 1.0\%$ oxygen. This suggests that the nanoparticles are represented by the polymer salt form, CTS aspartate.

4. Conclusions

In conclusion, cooperative interactions between fixed charges of the polycation and low-molecular counterions in the CTS – AspA – H₂O system are accompanied by the formation of ion pairs, multiplet structures, and phase segregation of the polymer substance to form nano- and microparticles. The "fixation" of the nuclei of a new phase at the initial stage of phase separation by injection spraying onto a glass support makes it possible to visualize the formation of particles by the SEM method. Further search for ways to stabilize particles in solution, for example, by creating a "shell" that prevents aggregation, will make it possible to develop methods for their preparation in a preparative amount. Due to the high biological activity of CTS and AspA, chitosan-containing nano- and microparticles can be promising as independent pharmaceutical and veterinary drugs, plant protection products, providing synergy of useful properties of their constituent components, as well as in drug storage and delivery systems, and therapeutics.

Acknowledgements

This work was financially supported by the Foundation for Assistance to Innovations of the Russian Federation (Grant No. 16317GU/2021).

References

- Li Q, Song B, Yang Z, Fan H. Electrolytic conductivity behaviors and solution conformations of chitosan in different acid solutions. *Carbohydr Polym*. 2006;63(2):272–282. doi:[10.1016/j.carbpol.2005.09.024](https://doi.org/10.1016/j.carbpol.2005.09.024)
- Bobreshova OV, Bobylkina OV., Kulintsov PI, Bobrinskaya GA, Varlamov VP, Nemtsev SV. Conductivity of aqueous solutions of low-molecular chitosan. *Russ J Electrochem*. 2004;40(7):694–697. doi:[10.1023/B:RUEL.0000035250.54523.e8](https://doi.org/10.1023/B:RUEL.0000035250.54523.e8)
- Osman Z, Ibrahim Z, Arof A. Conductivity enhancement due to ion dissociation in plasticized chitosan based polymer electrolytes. *Carbohydr Polym*. 2001;44(2):167–173. doi:[10.1016/S0144-8617\(00\)00236-8](https://doi.org/10.1016/S0144-8617(00)00236-8)
- Liu C-Y, Zhao K-S. Dielectric relaxations in chitosan solution with varying concentration and temperature: analysis coupled with a scaling approach and thermodynamical functions. *Soft Matter*. 2010;6(12):2742–2750. doi:[10.1039/B922807A](https://doi.org/10.1039/B922807A)
- Kasaai MR, Arul J, Charlet G. Fragmentation of Chitosan by Acids. *Sci World J*. 2013;508540:1–11. doi:[10.1155/2013/508540](https://doi.org/10.1155/2013/508540)
- Holme HK, Davidsen L, Kristiansen A, Smidsrod O. Kinetics and Mechanisms of Depolymerization of Alginate and Chitosan in Aqueous Solution. *Carbohydr Polym*. 2008;73(4):656–664. doi:[10.1016/j.carbpol.2008.01.007](https://doi.org/10.1016/j.carbpol.2008.01.007)
- Il'Ina AV, Varlamov VP. Hydrolysis of chitosan in lactic acid. *Appl Biochem Microbiol*. 2004;40(3):300–303. doi:[10.1023/B:ABIM.0000025956.98250.30](https://doi.org/10.1023/B:ABIM.0000025956.98250.30)
- Boyko IS, Podkolodnaya OA, Lysachok SG, Shmakov SL. Viscous Degradation of Acidic Chitosan Solutions and its Ionic Probe Study. *Izvestiya of Saratov University. Chem Biol Ecol*. 2015;15(4):21–30 (in Russian). doi:[10.18500/1816-9775-2015-15-4-21-30](https://doi.org/10.18500/1816-9775-2015-15-4-21-30)
- Philippova OE, Korchagina EV. Chitosan and its hydrophobic derivatives: Preparation and aggregation in dilute aqueous solutions. *Polym Sci Ser A*. 2012;54(7):552–572. doi:[10.1134/S0965545X12060107](https://doi.org/10.1134/S0965545X12060107)
- Chen RH, Chen WY, Wang ST, Hsu CH, Tsai ML. Changes in the Mark–Houwink hydrodynamic volume of chitosan molecules in solution of different organic acids, at different temperatures and ionic strengths. *Carbohydr Polym*. 2009;78(4):902–907. doi:[10.1016/j.carbpol.2009.07.027](https://doi.org/10.1016/j.carbpol.2009.07.027)
- Sorlier P, Viton C, Domard A. Relation between Solution Properties and Degree of Acetylation of Chitosan: Role of Aging. *Biomacromol*. 2002;3(6):1336–1342. doi:[10.1021/bm0256146](https://doi.org/10.1021/bm0256146)
- Fomina VI, Solonina NA, Shipovskaya AB. Ionic Aggregation of Macromolecules as the Cause of the Kinetic (Non) Stability of Physicochemical Properties of Chitosan Solutions. *Izvestiya of Saratov University. Chem Biol Ecol*. 2019;19(1):22–38 (in Russian). doi:[10.18500/1816-9775-2019-19-1-22-38](https://doi.org/10.18500/1816-9775-2019-19-1-22-38)
- Cavallaro G, Micciulla S, Chiappisi L, Lazzara G. Chitosan-based smart hybrid materials: A physico-chemical perspective. *J Mater Chem B*. 2021;9(3):594–611. doi:[10.1039/D0TB01865A](https://doi.org/10.1039/D0TB01865A)
- Zhou L, Ramezani H, Sun M, Xie M, Nie J, Lv S, He Y. 3D printing of high-strength chitosan hydrogel scaffolds without any organic solvents. *Biomater Sci*. 2020;8(18):5020–5028. doi:[10.1039/D0BM00896F](https://doi.org/10.1039/D0BM00896F)
- Hu L, Sun Y, Wu Y. Advances in chitosan-based drug delivery vehicles. *Nanoscale*. 2013;5(8):3103–3111. doi:[10.1039/C3NR00338H](https://doi.org/10.1039/C3NR00338H)
- Jhaveri J, Raichura Z, Khan T, Momin M, Omri A. Chitosan nanoparticles-insight into properties, functionalization and applications in drug delivery and therapeutics. *Mol*. 2021;26(2):272. doi:[10.3390/molecules26020272](https://doi.org/10.3390/molecules26020272)
- Garavand F, Cacciotti I, Vahedikia N, Salara AR, Tarhan Ö, Akbari-Alavijeh S., Shaddel R, Rashidinejad A, Nejatian M, Jafarzadeh S., Azizi-Lalabadi M, Khoshnoudi-Nia S, Jafari SM. A comprehensive review on the nanocomposites loaded with chitosan nanoparticles for food packaging. *Crit Rev Food Sci Nutr*. 2020;1–34. doi:[10.1080/10408398.2020.1843133](https://doi.org/10.1080/10408398.2020.1843133)
- Mohammed MA, Syeda J, Wasan KM, Wasan EK. An overview of chitosan nanoparticles and its application in non-parenteral drug delivery. *Pharm*. 2017;9(4):53. doi:[10.3390/pharmaceutics9040053](https://doi.org/10.3390/pharmaceutics9040053)
- Shafabakhsh R, Yousefi B, Asemi Z, Nikfar B, Mansournia MA, Hallajzadeh J. Chitosan: a compound for drug delivery system in gastric cancer-a review. *Carbohydr Polym*. 2020;242:116403. doi:[10.1016/j.carbpol.2020.116403](https://doi.org/10.1016/j.carbpol.2020.116403)
- Lang X, Wang T, Sun M, Chen X, Liu Y. Advances and applications of chitosan-based nanomaterials as oral delivery carriers: A review. *Int J Biol Macromol*. 2020;154:433–445. doi:[10.1016/j.ijbiomac.2020.03.148](https://doi.org/10.1016/j.ijbiomac.2020.03.148)
- Carrouel F, Viennot S, Ottolenghi L, Gaillard C, Bourgeois D. Nanoparticles as Anti-Microbial, Anti-Inflammatory, and Remineralizing Agents in Oral Care Cosmetics: A Review of the

- Current Situation. *Nanomater.* 2020;10(1):140. doi:[10.3390/nano10010140](https://doi.org/10.3390/nano10010140)
22. Li D, Karsl B, Rubio NK, Janes M, Luo Y, Prinyawiwatkul W, Xu W. Enhanced microbial safety of channel catfish (*Ictalurus punctatus*) fillet using recently invented medium molecular weight water-soluble chitosan coating. *Lett Appl Microbiol.* 2020;70(5):380–387. doi:[10.1111/lam.13284](https://doi.org/10.1111/lam.13284)
 23. Ahmed TA, Aljaeid BM. Preparation, characterization, and potential application of chitosan, chitosan derivatives, and chitosan metal nanoparticles in pharmaceutical drug delivery. *Drug Des Dev Ther.* 2016;10:483–507. doi:[10.2147/DDDT.S99651](https://doi.org/10.2147/DDDT.S99651)
 24. Bagheri M, Younesi H, Hajati S, Borghe SM. Application of chitosan–citric acid nanoparticles for removal of chromium (VI). *Int J Biol Macromol.* 2015;80:431–444. doi:[10.1016/j.jbiomac.2015.07.022](https://doi.org/10.1016/j.jbiomac.2015.07.022)
 25. Bodnar M, Hartmann JF, Borbely J. Preparation and characterization of chitosan-based nanoparticles. *Biomacromol.* 2005;6:2521–2527. doi:[10.1021/bm0502258](https://doi.org/10.1021/bm0502258)
 26. Roy SG, Shirsat NS, Mishra AC, Waghulde SO, Kale MK. A review on chitosan nanoparticles applications in drug delivery. *J Pharmacogn Phytochem.* 2018;7:1–4. doi:[10.22271/phyto.2018.v7.isp6.1.01](https://doi.org/10.22271/phyto.2018.v7.isp6.1.01)
 27. Sahariah P, Masson M. Antimicrobial chitosan and chitosan derivatives: a review of the structure–activity relationship. *Biomacromol.* 2017;18(11):3846–3868. doi:[10.1021/acs.biomac.7b01058](https://doi.org/10.1021/acs.biomac.7b01058)
 28. Zaboon MH, Saleh AA, Al-Lami HS. Synthesis, Characterization and Cytotoxicity Investigation of Chitosan-Amino Acid Derivatives Nanoparticles in Human Breast Cancer Cell Lines. *J Mex Chem Soc.* 2021;65(2):178–188. doi:[10.29356/imcs.v65i2.1265](https://doi.org/10.29356/imcs.v65i2.1265)
 29. Rossi S, Vigani B, Puccio A, Bonferoni MC, Sandri G, Ferrari F. Chitosan ascorbate nanoparticles for the vaginal delivery of antibiotic drugs in atrophic vaginitis. *Mar Drugs.* 2017;15(10): 319. doi:[10.3390/md15100319](https://doi.org/10.3390/md15100319)
 30. Yu J, Wang D, Geetha N, Khawar KM, Jogaiah S, Mujtaba M. Current trends and challenges in the synthesis and applications of chitosan-based nanocomposites for plants: A review. *Carbohydr Polym.* 2021;261:117904. doi:[10.1016/j.carbpol.2021.117904](https://doi.org/10.1016/j.carbpol.2021.117904)
 31. Salgado-Cruz MDLP, Salgado-Cruz J, García-Hernández AB, Calderón-Domínguez G, Gómez-Viquez H, Oliver-Espinoza R, Yáñez-Fernández J. Chitosan as a Coating for Biocontrol in Postharvest Products: A Bibliometric Review. *Membr.* 2021;11(6):421. doi:[10.3390/membranes11060421](https://doi.org/10.3390/membranes11060421)
 32. Divya K, Vijayan S, Nair SJ, Jisha MS. Optimization of chitosan nanoparticle synthesis and its potential application as germination elicitor of *Oryza sativa* L. *Int J Biol Macromol.* 2019;124:1053–1059. doi:[10.1016/j.jbiomac.2018.11.185](https://doi.org/10.1016/j.jbiomac.2018.11.185)
 33. Khaptsev Z, Lugovitskaya T, Shipovskaya A, Shipenok K. Biological activity of chitosan aspartate and its effect on germination of test seeds. *IOP Conf Ser: Earth Environ Sci.* 2021;723(2):022074. doi:[10.1088/1755-1315/723/2/022074](https://doi.org/10.1088/1755-1315/723/2/022074)
 34. Ayon NJ. Features, roles and chiral analyses of proteinogenic amino acids. *AIMS Mol Sci.* 2020;7(3):229–268. doi:[10.3934/molsci.2020011](https://doi.org/10.3934/molsci.2020011)
 35. Sang-Aroon W, Ruangpornvisuti V. Determination of aqueous acid-dissociation constants of aspartic acid using PCM/DFT method. *Int J Quantum Chem.* 2007;108(6):1181–1188. doi:[10.1002/qua.21569](https://doi.org/10.1002/qua.21569)
 36. Lee HS, Hong J. Electrokinetic separation of lysine and aspartic acid using polypyrrole-coated stacked membrane system. *J Membr Sci.* 2000;169(2):277–285. doi:[10.1016/S0376-7388\(99\)00349-X](https://doi.org/10.1016/S0376-7388(99)00349-X)
 37. Apelblat A, Manzurola E, Orekhova Z. Electrical conductance studies in aqueous solutions with aspartic ions. *J Solut Chem.* 2008;37(1):97–105. doi:[10.1007/s10953-007-9223-5](https://doi.org/10.1007/s10953-007-9223-5)
 38. Mondal S, Agam Y, Nandi R, Amdursky N. Exploring long-range proton conduction, the conduction mechanism and inner hydration state of protein biopolymers. *Chem Sci.* 2020;11(13): 3547–3556. doi:[10.1039/C9SC04392F](https://doi.org/10.1039/C9SC04392F)
 39. Lugovitskaya TN, Shipovskaya AB. Physicochemical properties of aqueous solutions of L-aspartic acid containing chitosan. *Russ J Gen Chem.* 2017;87(4):782–787. doi:[10.1134/S1070363217040193](https://doi.org/10.1134/S1070363217040193)
 40. Lugovitskaya TN, Zudina IV, Shipovskaya AB. Obtaining and Properties of L-Aspartic Acid Solutions of Chitosan. *Russian J Appl Chem.* 2020;93(1):80–88. doi:[10.1134/S1070427220010097](https://doi.org/10.1134/S1070427220010097)
 41. Volkov EV, Filippova OE, Khokhlov AR. Dual polyelectrolyte-ionomer behavior of poly (acrylic acid) in methanol: 1. salt-free solutions. *Colloid J.* 2004;66(6):663–668. doi:[10.1007/s10595-005-0044-1](https://doi.org/10.1007/s10595-005-0044-1)
 42. Kramarenko EY, Khokhlov AR. Effect of formation of ion pairs on the stability of stoichiometric block ionomer complexes. *Polym Sci Ser A.* 2007;49(9):1053–1063. doi:[10.1134/S09655445X07090131](https://doi.org/10.1134/S09655445X07090131)
 43. Cervera MF, Heinämäki J, de la Paz N, López O, Maunu SL, Virtanen T, Yliruusi J. Effects of spray drying on physico-chemical properties of chitosan acid salts. *Aaps Pharmscitech.* 2011;12(2):637–649. doi:[10.1208/s12249-011-9620-3](https://doi.org/10.1208/s12249-011-9620-3)